View metadata, citation and similar papers at core.ac.uk
brought to you by CORE
provided by NASA Technical Reports Server

N86-17842

FURTHER RESEARCH ON HIGH OPEN CIRCUIT VOLTAGE IN SILICON SOLAR CELLS*

M. B. Spitzer and C. J. Keavney
Spire Corporation
Bedford, Massachusetts

This paper presents the results of new research on the use of controlled dopant profiles and oxide passivation to achieve high open circuit voltage (V_{oc}) in silicon solar cells. In this work, ion implantation has been used to obtain nearly optimal values of surface dopant concentration. The concentrations are selected so as to minimize heavy doping effects and thereby provide both high blue response and high V_{oc}. Our ion implantation technique has been successfully applied to fabrication of both n-type and p-type emitters. V_{oc} of up to 660 mV is reported and AMO efficiency measured by NASA-LeRC of 16.1% has been obtained.

INTRODUCTION

The attainment of silicon solar cell conversion efficiency approaching the theoretical limit requires reduction of recombination in all volumes and at all surfaces of the cell (ref. 1). One method of reducing base recombination comprises the use of thin substrates and minority carrier reflecting surfaces of the type formed by $p\text{-}p^+$ junctions (ref. 1, 2). However, achievement of the very highest performance requires minimal recombination not only in the base region, but also in the p^+ region and at the p^+/contact interface. Moreover, as the base is perfected, recombination in the n^+ emitter and at its surface emerges as a limiting mechanism and must also be minimized. Thus, one general prerequisite to the attainment of high efficiency is the perfection of n^+ and p^+ regions that, while remaining useful for junction formation, introduce only minimal recombination. Following Shibib at al. (ref. 3), we call these low recombination doped regions "transparent."

To effectively utilize transparent regions in solar cells, passivation must be applied to the cell surface (ref. 4). Although in theory the construction of a transparent passivated structure appears straightforward, in practice such structures are not so easily fabricated. Some of the difficulties arise as a consequence of the need to limit heavy-doping effects to obtain transparency. Also, as has been noted by others, recombination at the interface between the silicon and the metal contact must be minimized (ref. 5-8). These factors conspire to make the attainment of low recombination (and resultant high V_{oc}) using conventional cell fabrication techniques rather difficult.

---

* This work has been supported by the U.S. Department of Energy through contracts with the Solar Energy Research Institute and Sandia National Laboratories.

In this paper, we present the results of research on fabrication techniques that minimize heavy-doping effects and surface recombination. In the work to be reported, we have used ion implantation to vary over a wide range dopant concentration in both phosphorus-doped n^+ regions and boron-doped p^+ regions. Unlike conventional diffusion, in which the surface dopant concentration is usually quite high ($\sim 10^{20} cm^{-3}$), in our technique, the number of ions implanted can be easily varied to achieve concentrations from about $10^{18} cm^{-3}$ to over $10^{20} cm^{-3}$. A further advantage of ion implantation is that a high quality surface oxide of controllable thickness may be easily grown during the junction anneal. As we will show, this technique has yielded AMO V_{OC} of 660 mV, without the use of an antireflection (AR) coating (which would increase V_{OC} by at least 7mV).

In the next section of this paper, we will describe our method and cell fabrication techniques. This will be followed by separate discussions of experiments with n^+ and p^+ doping, and results on high efficiency cells will be reported. In the conclusion we review the implications of this work in future space solar cell design.

CELL FABRICATION

All work to be reported here is based on the use of float-zone silicon obtained from Wacker. The wafers were 380 micrometers (μm) in thickness, polished on the front and etched on the back, and were of <100> orientation. Except as noted in the discussion to follow, the resistivity was 0.3 ohm-cm. Both boron-doped and phosphorus-doped wafers were used. We observed that the boron-doped wafers typically had a minority carrier diffusion length (L_D) of about 150 μm; the phosphorus-doped wafers were characterized by L_D of about 170 μm. While for space solar cell applications we are primarily interested in a p-type base, the use of n-type wafers provides us with a convenient method of investigating p^+ doping (i.e., by formation of p^+n cells) and the advantages of this approach will become apparent in the discussion to follow.

The n^+ and p^+ regions were formed by ion implantation and furnace annealing. The implantation of boron and phosphorus was carried out at 5 keV to obtain shallow junctions ($x_j \sim 0.2 \mu m$). The dose was varied over the range $10^{14} cm^{-2}$ to $5x10^{15} cm^{-2}$ to produce doping profiles having a peak concentration of between $10^{18} cm^{-3}$ and $10^{20} cm^{-3}$. Annealing of phosphorus was carried out using a three-step process (550°C-2 hr.; 850°C-15 min.; 550°C-2 hr.) in dry flowing nitrogen. Dry oxygen was admitted to the gas stream during the second step to grow a passivating silicon dioxide surface layer having a thickness of about 10 nanometers (nm). Annealing of boron implants was similar, with the exception that the second step of the anneal was carried out at 950°C.

Metallization on all cells comprised lift-off patterned Ti-Pd-Ag on the fronts and full-area Ti-Pd-Ag on the backs. The metal was deposited by electron beam evaporation, and after lift-off was plated with Ag. Except as noted, AR coatings were not employed. Final cell area was 4 cm^2.

An important feature that we shall refer to later in our discussion is the use of silicon dioxide surface passivation, both at the exposed (non-metallized) surface and beneath the metallization. While some

investigators have employed tunneling-based passivation beneath the contacts, we have used an older approach previously employed by Minnucci and Matthei (ref. 8) and Arndt et al. (ref. 6). The technique comprises placing the grid on top of the passivating oxide, with ohmic contact made via patterned openings in the oxide. These openings limit contact area to values much less than the total grid area. Figure 1 illustrates two configurations that have been used to achieve this end. These techniques allow us to limit the ohmic contact area to 0.1 percent of the total area.

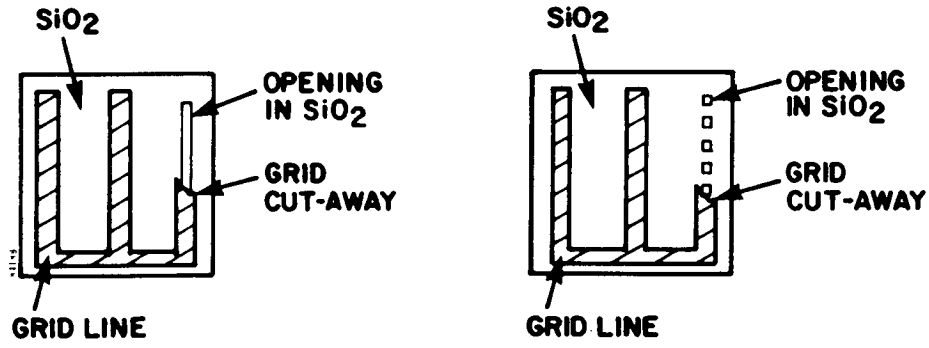

Figure 1. Two Configurations for Limiting Ohmic Contact Area Beneath the Front Contact Grid.

PHOSPHORUS EMITTER DOPING

We have used the ion implantation technique described above to identify the optimum n^+ concentration in the emitter of n^+-p-p^+ cells. Figure 2 replicates spreading resistance data obtained from samples that were ion-implanted with various doses. It can be seen that by using the ion implantation technique, the peak dopant concentration may be varied over a wide range.

Solar cells were fabricated with each of the profiles shown in Figure 2 and early results of this type of research were reported in reference 9. We recently repeated the experiment with a narrower range of doses and show the V_{oc} as a function of phosphorus implant dose in figure 3 for both 0.2 ohm-cm (curve b) and 0.3 ohm-cm (curve c) substrates. It is important to note that ohmic contact interaction area was about 4% in this experiment. Complete data is tabulated in tables I and II. It can be seen that best results are obtained with an ion implantation dose of 10^{15} ions/cm^2, corresponding to a peak dopant concentration of approximately 2 x 10^{19}cm^{-3}.

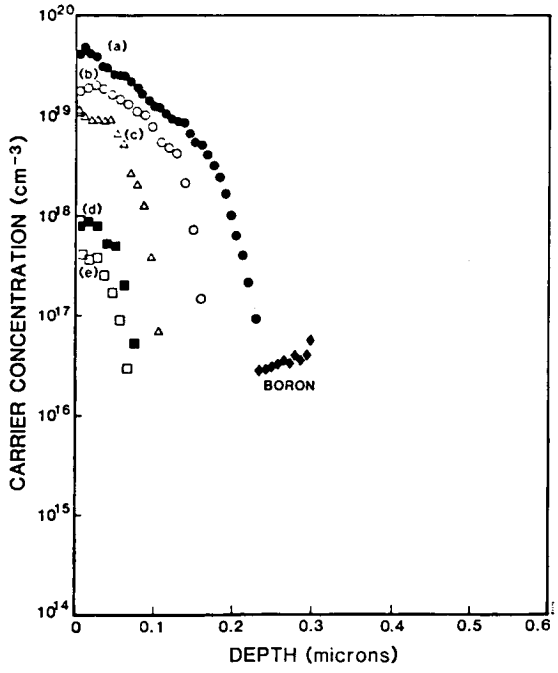

Figure 2. Spreading Resistance Analysis of n^+ Emitters. The doses used were: (a) $2.5 \times 10^{15} cm^{-2}$, (b) $10^{15} cm^{-2}$, (c) $4 \times 10^{14} cm^{-2}$, (d) $2 \times 10^{14} cm^{-2}$, and (e) $10^{14} cm^{-2}$.

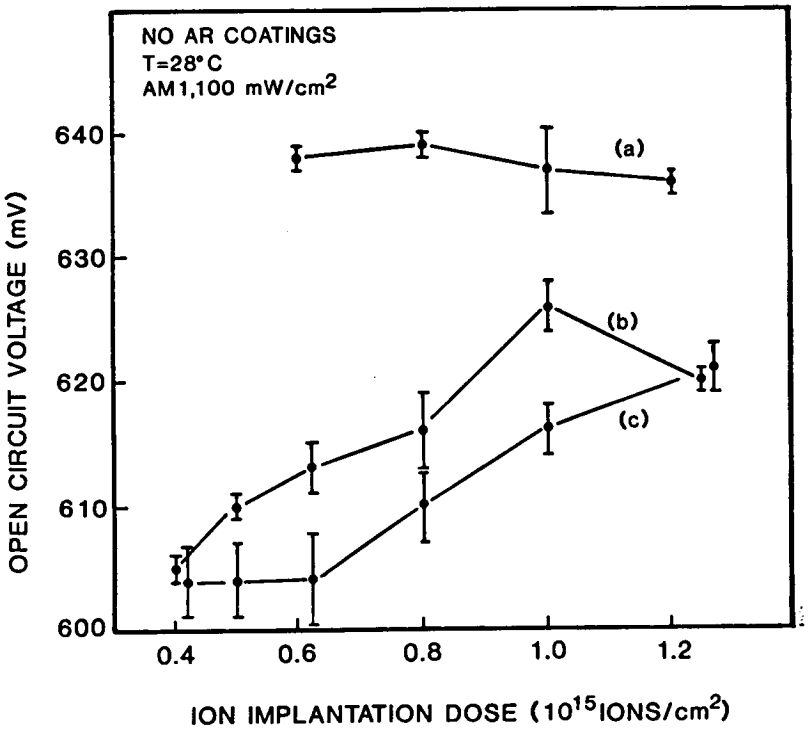

Figure 3. V_{OC} as a function of ion implantation dose. The data points indicate average V_{OC} at each dose. The error bars indicate the standard deviation. (Measurements at AM1, 100 mW/cm^2, T=28°C).

We digress at this point to note our observation that the minority carrier diffusion length in the base is strongly affected by the phosphorus concentration in the emitter. An example of this effect can be seen in tables I and II in which we have also indicated the base L_D for each ion implantation dose. We find a reproducible decrease in L_D as dose is decreased. This effect cannot be attributed to implantation of a lifetime degrading impurity, since in such a case increasing the phosphorus dose would increase the lifetime degrading impurity and decrease L_D. Perhaps it is an indication of phosphorus gettering; however, the source of the lifetime degrading impurities is uncertain. Indeed, laser-annealed cells in which no thermal processing is used and in which no gettering is possible have yet higher L_D. Experiments that combine Si implantation with P implantation to maintain constant implant damage as the P dose is reduced indicate that the observed effect is not a consequence of differences in the crystal damage. The same effect is observed with arsenic implantation, but not with boron. The cause of the observed effect is unresolved.

To identify the optimal ion implantation dose more accurately, we repeated the above dose experiment with implantation dose in a range from $6x10^{14}cm^{-2}$ to $1.2x10^{15}cm^{-2}$. We utilized silicon with a base resistivity of 0.2 ohm-cm to maintain a low base contribution to the saturation current. We also reduced the ohmic contact area (as shown in figure 1) to 0.1 percent. The V_{oc} data are shown in figure 2 (curve a). The resultant complete cell performance data are shown in table III. The average V_{oc} is maximized at a dose of $8x10^{14}cm^{-2}$; however V_{oc} greater or equal to 640 mV on at least one cell at each dose except $1.2x10^{15}cm^{-2}$ was obtained. Comparison of this data to data in table I indicates the advantage that is obtained when ohmic contact interaction area is limited.

We have also applied these implants to textured wafers and have recently reported on an estimation of the dopant distribution in textured material (ref. 10). Our principal finding is that dopant distributions that are equivalent to distributions in polished silicon may be obtained in textured silicon by simply doubling the implantation dose. In this way, we have made textured cells with V_{oc} of 640 mV, equivalent to V_{oc} obtained from polished wafers. This indicates to us that the base saturation current dominates our best cells, since the emitter saturation current, which is higher for textured cells, does not adversely affect V_{oc} when texture is used.

The emitters described above have been applied in the fabrication of high efficiency cells. One cell that was tested under AM0 insolation ($137.2\ mW/cm^2$) at NASA-LeRC exhibited the following performance: FF=0.796, J_{sc}=43.5 mA/cm^2, V_{oc}=640 mV, and Eff.=16.1%. This cell had a thickness of 380 μm, and a diffusion length of about 150 μm. We believe that its performance can be further improved by thinning the substrate to 200 μm. For this approach to be successful, a high quality back surface field (BSF) must be employed. We will describe in a later section how such a BSF may be formed.

TABLE I
AVERAGE AM1 PERFORMANCE OF P-TYPE SOLAR CELLS AS A FUNCTION OF ION IMPLANTATION DOSE (0.2 OHM-CM SUBSTRATES)

Dose (ions/cm^2)	L_D (μm)	V_{oc} (mV)	J_{sc} (mA/cm^2)	FF (%)	EFF (%)
$4x10^{14}$	63	605 (1)	21.7 (0.2)	78.8 (0.2)	10.3 (0.2)
$5x10^{14}$	77	610 (1)	21.9 (0.2)	79.2 (2.0)	10.6 (0.3)
$6.25x10^{14}$	85	613 (3)	22.1 (0.2)	79.0 (1.7)	10.7 (0.3)
$8x10^{14}$	90	616 (3)	22.4 (0.2)	79.9 (0.9)	11.0 (0.2)
$1x10^{15}$	138	626 (2)	23.8 (0.2)	79.2 (1.9)	11.8 (0.3)
$1.25x10^{15}$	137	620 (1)	23.7 (0.2)	78.5 (1.4)	11.6 (0.3)

Notes: Cell area is 4 cm^2. Insolation is simulated AM1, 100 mW/cm^2. T = 28°C. Standard deviation in parenthesis. No AR coatings employed.

TABLE II
AVERAGE AM1 PERFORMANCE OF P-TYPE SOLAR CELLS AS A FUNCTION OF ION IMPLANTATION DOSE (0.3 OHM-CM SUBSTRATES)

Dose (ions/cm^2)	L_D (μm)	V_{oc} (mV)	J_{sc} (mA/cm^2)	FF (%)	EFF (%)
$4x10^{14}$	60	604 (3)	21.8 (0.2)	80.3 (0.4)	10.6 (0.1)
$5x10^{14}$	77	604 (3)	22.0 (0.1)	78.9 (1.1)	10.5 (0.2)
$6.25x10^{14}$	74	604 (4)	22.0 (0.3)	79.5 (1.4)	10.5 (0.3)
$8x10^{14}$	95	610 (3)	22.5 (0.3)	80.4 (1.0)	11.0 (0.3)
$1x10^{15}$	133	616 (2)	23.5 (0.2)	79.7 (0.8)	11.5 (0.2)
$1.25x10^{15}$	150	621 (2)	24.2 (0.1)	80.9 (0.6)	12.2 (0.1)

Notes: Cell area is 4 cm^2. Insolation is simulated AM1, 100 mW/cm^2. T = 28°C. Standard deviation in parenthesis. No AR coatings employed.

TABLE III
AVERAGE AM1 PERFORMANCE OF P-TYPE SOLAR CELLS WITH IMPROVED CONTACTS AS A FUNCTION OF ION IMPLANTATION DOSE (0.2 OHM-CM SUBSTRATES)

Dose (ions/cm^2)	L_D (μm)	V_{oc} (mV)	J_{sc} (mA/cm^2)	FF (%)	EFF (%)
$6x10^{14}$	67	638 (1)	22.0 (0.3)	79.0 (1.3)	11.1 (0.3)
$8x10^{14}$	101	639 (1)	23.1 (0.1)	78.4 (1.5)	11.6 (0.3)
$1x10^{15}$	119	637 (4)	23.6 (0.2)	79.8 (0.8)	12.0 (0.2)
$1.2x10^{15}$	118	636 (1)	23.6 (0.1)	80.0 (1.4)	12.0 (0.2)

Notes: Cell area is 4 cm^2. Contact interaction area is 0.1%. Insolation is simulated AM1, 100 mW/cm^2. T = 28°C. Standard deviation in parenthesis. No AR coatings employed.

BORON EMITTER DOPING

A similar investigation has been carried out using boron implantation into n-type wafers. A beam energy of 5 keV was used to obtain shallow junctions. Implantation doses in the range of $3x10^{14}cm^{-2}$ to $1x10^{15}cm^{-2}$ were used to obtain peak dopant concentrations of between $5x10^{18}cm^{-3}$ and $10^{19}cm^{-3}$. It can be seen from the spreading resistance analysis in figure 4 that dopant profiles similar to those that have been used for phosphorus emitters have been attained.

Solar cells have been fabricated from n-type wafers using the profiles shown in figure 4. We have investigated both standard ohmic contacts and contacts with ohmic contact interaction area reduced to 0.1%, and complete cell performance data are shown in table IV. It can be seen that best V_{oc} is obtained when the peak doping concentration is limited to about $5x10^{18}$ cm^{-3}. As in the case of n^+ emitters, reduction of ohmic contact area improves V_{oc}. Note also that the FF is reduced when the ohmic contact area is reduced. This low FF is attributable to the use of Ti-Pd-Ag contacts on the p^+ silicon and arises from contact series resistance. Use of Al would probably eliminate this problem.

High V_{oc} n-type cells have also been tested at AM0 by NASA-LeRC. Performance of the best non-AR-coated cell is: J_{sc}=28.8 mA/cm^2, FF=.77, V_{oc}=662 mV, and Eff.=10.7%. An AR coating would improve efficiency to about 15%, and V_{oc} to nearly 670 mV.

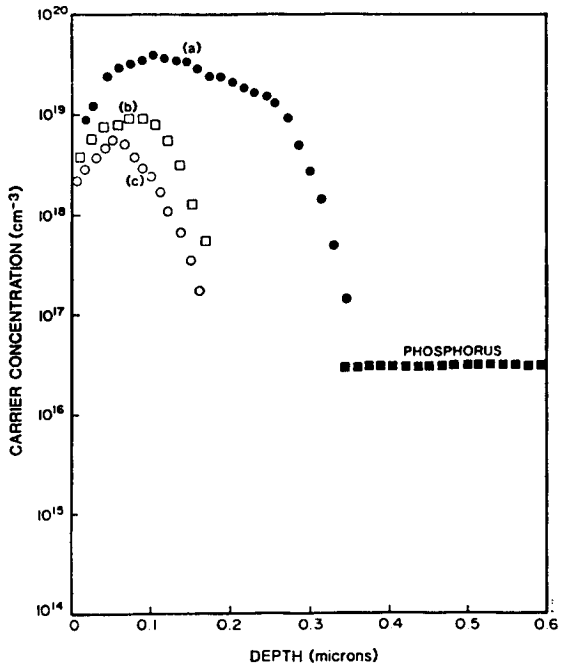

Figure 4. Spreading Resistance Analysis of p^+ Emitters. The doses used were: (a) $1x10^{15}cm^{-2}$, (b) $5x10^{14}cm^{-2}$, and (c) $3x10^{14}cm^{-2}$.

TABLE IV
AVERAGE AM1 PERFORMANCE OF N-TYPE SOLAR CELLS
AS A FUNCTION OF ION IMPLANTATION DOSE (0.3 OHM-CM SUBSTRATES)

Dose (ions/cm^2)	Contact Interaction Area	V_{oc} (mV)	J_{sc} (mA/cm^2)	FF (%)	EFF (%)
$3x10^{14}$	0.1%	653 (1)	24.7 (0.1)	73.8 (2.8)	11.9 (0.5)
$3x10^{14}$	4%	634 (3)	24.6 (0.1)	77.7 (3.4)	12.1 (0.6)
$5x10^{14}$	0.1%	644 (2)	24.6 (0.1)	78.3 (1.0)	12.4 (0.2)
$5x10^{14}$	4%	634 (2)	24.6 (0.1)	78.6 (1.5)	12.3 (0.3)
$1x10^{15}$	4%	591 (2)	22.2 (0.1)	79.7 (1.8)	10.5 (0.3)

Notes: Cell area = 4 cm^2. Insolation was AM1, 100 mW/cm^2. T = 28°C. Standard deviation shown in parenthesis. No AR coatings employed.

It is interesting that better V_{oc} is obtained with n-type wafers. This may be a consequence of the lower minority carrier (hole) mobility in n-type silicon which would serve to reduce the base saturation current.

TRANSPARENT REGIONS

To show conclusively that we have attained transparent emitter regions, we have examined solar cell performance with and without silicon dioxide passivation. Figure 5 replicates log(I)-V data obtained from one n^+-p-p^+ solar cell before and after removal of the oxide. It can be seen that the saturation (or dark) current increases in accordance with theory when the oxide is removed. The change in V_{oc} upon removal of the oxide was 47 mV. In figure 6 we show the quantum efficiency data, before and after oxide removal. It is clear from this data that the blue response is much improved by the presence of the oxide.

Figure 7 replicates log(I)-V data for a typical p^+-n-n^+ solar cell. Removal of the oxide increases the saturation current as it did in the n^+-p-p^+ example. In this case the change in V_{oc} was 75 mV. Quantum efficiency data (fig. 8) show that the blue response is also sensitive to surface recombination. These measurements indicate that we have indeed formed transparent n^+ and p^+ regions.

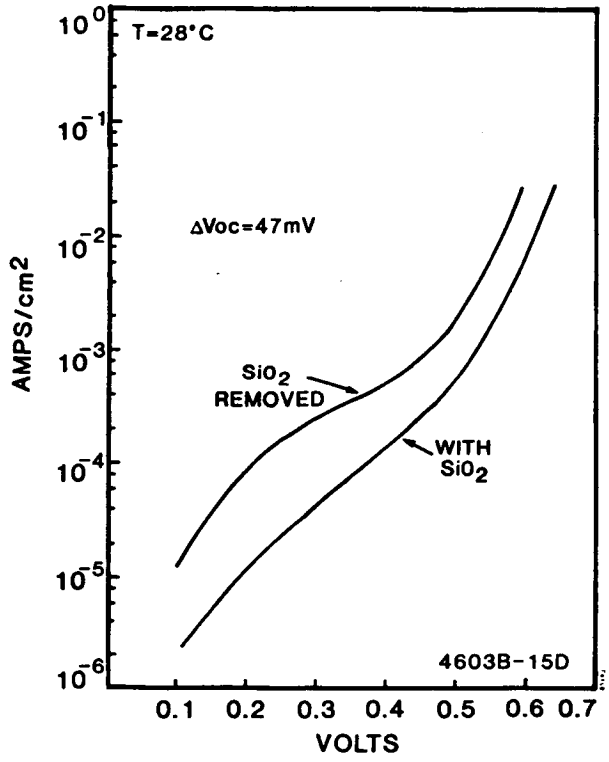

Figure 5. Log(I)-V Data for the n^+-p-p^+ Cell With and Without Oxide Passivation.

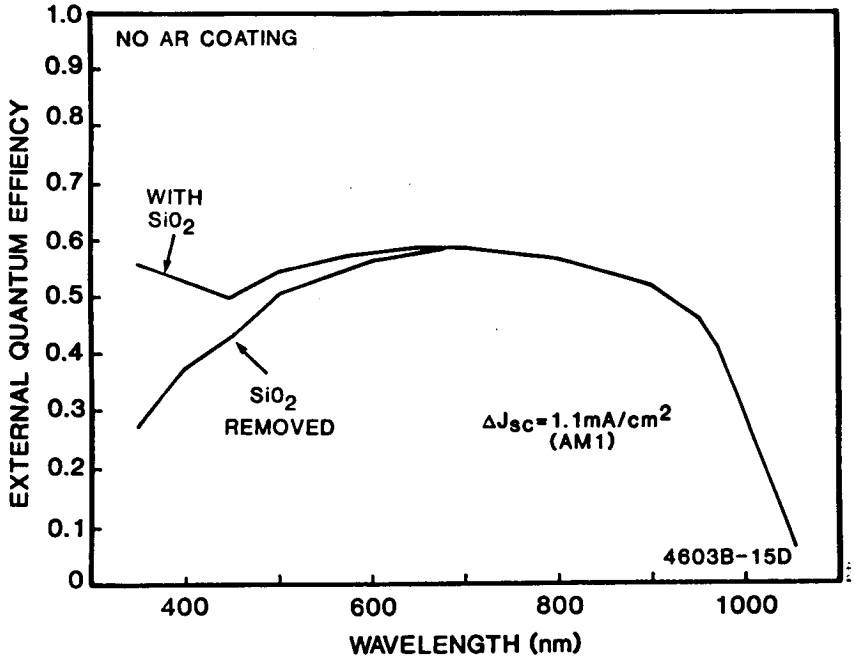

Figure 6. External Quantum Efficiency of the n^+-p-p^+ Cell With and Without Oxide Passivation.

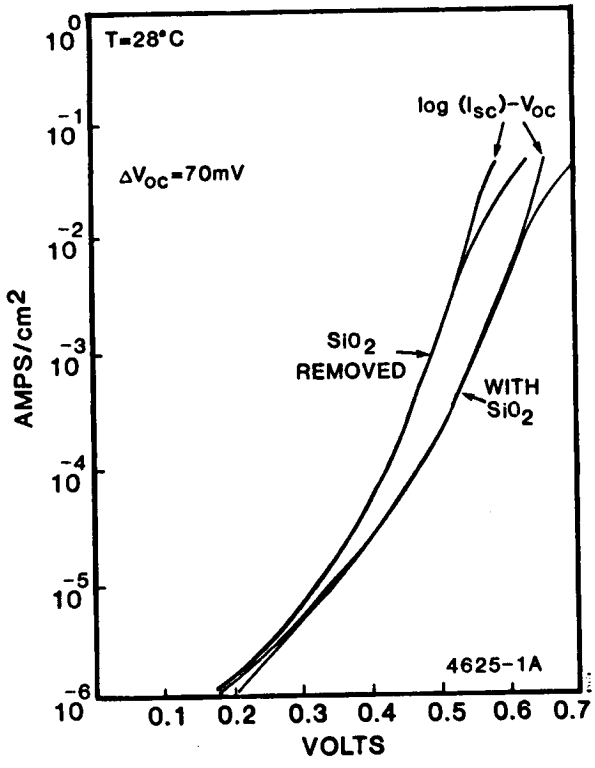

Figure 7. Log(I)-V Data for the p^+-n-n^+ Cell With and Without Oxide Passivation. Also shown are Log (I_{sc})-V_{oc} Data.

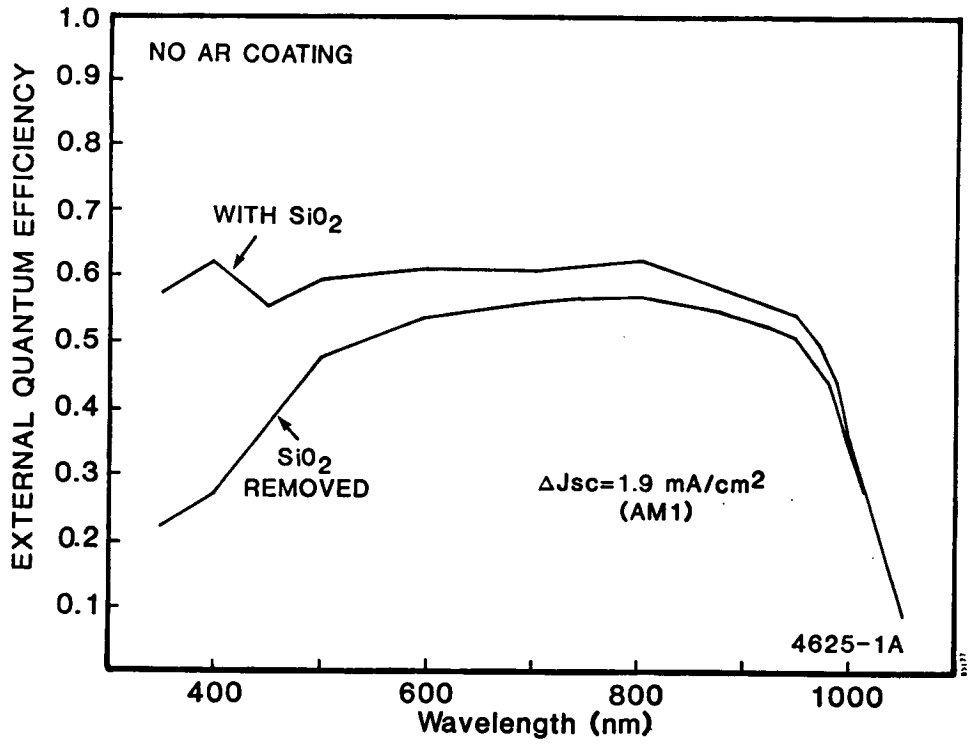

Figure 8. External Quantum Efficiency of the p^+-n-n^+ Cell With and Without Oxide Passivation.

HIGH EFFICIENCY CELL DESIGN

As was noted at the beginning of this paper, the attainment of high conversion efficiency requires limiting all forms of recombination. The best cell design should therefore include low-recombination transparent doped regions and surface passivation. This idea is of course not new, but we now have in hand a fabrication process that, by using ion implantation, will let us realize such doped regions.

Figure 9 illustrates the cell design we believe at this time will yield best performance. The device comprises an n^+-p-p^+ structure with the n^+ and p^+ regions formed by the transparent doped layers discussed above. Total thickness should be less than 250 μm, but the optimal value will depend upon the diffusion length in the substrate. A back surface reflector should be used to double the optical path and to reject unabsorbed radiation. Since the back surface has low recombination velocity, the cell may be made as thin as is desired for weight reasons, without loss of V_{oc}. At present, we are in the process of developing this type of cell. If light-trapping can be obtained (ref. 2), very high efficiency will be possible using substrates as thin as 50μm.

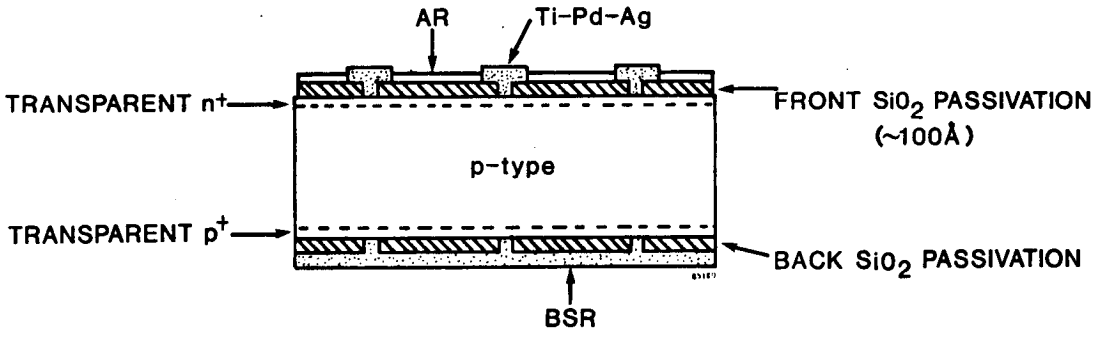

Figure 9. High Efficiency Space Solar Cell Design.

SUMMARY

This paper has reported on techniques that may be used to avoid heavy doping effects in silicon solar cells. In this way, transparent n^+ and p^+ layers have been formed. By combining these layers with silicon dioxide passivation, solar cells that are mainly limited by base recombination can be fabricated. Once this is accomplished, the problem of improving solar cell efficiency is reduced to gaining improvements in L_D, or alternately, to thinning of the substrate. Proper integration of these results in a BSF-BSR cell design should lead to AM0 efficiency in the 17 to 18% range in the near future.

REFERENCES

1. Wolf, M.: Updating the Limit Efficiency of Silicon Solar Cells. IEEE Trans. Electron Devices ED-27, 751 (1980).

2. Spitzer, M., Shewchun, J., Loferski, J.J., and Vera, E.S.: Ultra High Efficiency Thin Silicon p-n Junction Solar Cells Using Reflecting Surfaces. Rec. of the 14th IEEE Photovoltaic Specialists Conference (1980) p. 375.

3. Shibib, M.A., Lindholm, F.A., and Therez, F.: Heavily Doped Transparent-Emitter Regions in Junction Solar Cells, Diodes, and Transistors. IEEE Trans. Electron Devices ED-26, 959 (1979).

4. Fossum, J.G., Lindholm, F.A., and Shibib, M.A.: The Importance of Surface Recombination and Energy-bandgap Narrowing in p-n-junction Silicon Solar Cells. Trans. Electron Devices ED-26, 1294 (1979).

5. Lindholm, F.A., Mazer, J.A., Davis, J.R., and Perreota, J.T.: Degradation of Solar Cell Performance by Areal Inhomogeneity. Solid-State Electronics 23, 967 (1980).

6. Arndt, R.A., Meulenberg, A., Allison, J.F.: Advances in High Output Voltage Silicon Solar Cells. Rec. of the 15th IEEE Photovoltaic Specialists Conference, 1981, p. 92.

7. Green, M.A., Blakers, A.W., Shi, J., Keller, E.M. and Wenham, S.R.: 19.1% Efficient Silicon Solar Cell. Appl. Phys. Lett. 44, 1163 (1984).

8. Minnucci, J.A., and Matthei, K.W.: Study Program to Improve the Open-Circuit Voltage of Low Resistivity Single Crystal Silicon Solar Cells. NASA CR-159833 (1980).

9. Spitzer, M.B., Keavney, C.J., Tobin, S.P., Lindholm, F.A. and Neugroschel, A.: Mechanisms Limiting Open Circuit Voltage in Silicon Solar Cells. Rec. of the 17th IEEE Photovoltaic Specialists Conference, 1984, p. 1218.

10. Keavney, C.J., and Spitzer, M.B.: Solar Cell Junction Profiles in Ion-Implanted Texture-etched Surfaces. J. Appl. Phys. 56, 592 (1984).